GROUNDWATER QUALITY ASSESSMENT IN SEMI ARID REGIONS USING INTEGRATED APPROACHES: THE CASE OF GROMBALIA AQUIFER (NE TUNISIA)

Siwar Kammoun [a,*], Rim Trabelsi [a], Viviana Re [a, b], Kamel Zouari [a], Jihed Henchiri [a]

[a] *Laboratory of Radio-Analyses and Environment, National School of Engineers of Sfax, BP1173, 3038 Sfax, Tunisia*

Email: siwarkammoun@gmail.com

[b] *Department of Molecular Sciences and Nanosystems, Ca' Foscari University of Venice.CalleLarga Santa Marta 2137 –Dorsoduro 40123 Venice, Italy*

Abstract

As many arid and semi-arid regions in the Mediterranean basin, the Grombalia coastal aquifer (NE Tunisia) is affected by increasing groundwater exploitation and quality depletion. Therefore, quality assessments are becoming increasingly important as the long-term protection of water resources is at stake. Multidisciplinary investigations, like the one presented in this paper, are particularly effective in identifying the different origins of mineralization within an aquifer and investigating the impact of agricultural and anthropogenic activities on groundwater quality, especially in semi arid coastal regions. Groundwater quality assessment, focused on the combined use of geostatistical, hydrogeochemical and isotopic tools ($\delta^{18}O$, δ^2H and ^3H), was performed in the Grombalia aquifer between February and March 2014 to study the main processes controlling aquifer salinization, with special attention to anthropogenic contamination. Results indicate a persisting deterioration of water quality over the whole study area, except in the South-eastern zone juxtaposing the recharge boundary of the aquifer. Nitrate contents exceed the WHO drinking water standard (50 mg/l) in 70% of groundwater samples, mainly due to the excessive use of fertilizers and urban activities. Stable isotopes measurements showed the contribution of modern rainwater to groundwater recharge, and proved the presence of evaporation contributing to the salinity increase. Tritium values in the groundwater samples suggested two hypotheses: the existence of mixture between old and recent water or/and the existence of two recharge periods of the aquifer, pre and post nuclear weapons test. Principal components analysis (PCA) confirmed the geochemical interpretation, highlighting that water-rock interaction, evaporation effect, and intensive anthropogenic activities (e.g. agricultural practices) constitute the main processes controlling the regional groundwater mineralization.

Keywords: groundwater, isotopes, geostatistics, mineralization, nitrate pollution.

1. Introduction

Groundwater is the main source of renewable fresh water for many Mediterranean countries, especially in the arid and semi-arid coastal zones of Southern Europe, the Middle East and North Africa Region (Re and Zuppi 2011). In these areas the rapid population growth and the associated intensive economic activities results in a severe increase in water demand (Zghibi et al. 2013; Machiwal and Jha 2015), leading to often excessive

groundwater exploitation (Paniconi et al. 2001; Giordano 2009; Siebert et al. 2010; Van der Gun 2012). This is why water scarcity is becoming an important concern, in both urban and rural zones along the Mediterranean, where groundwater is intensively used for irrigation and domestic consumption (Edmunds 2009; GWP 2012; UNESCO-ISARM 2004; Zuppi 2008). In addition to the emergence of water scarcity issues, groundwater quality degradation is also threatening the natural conditions of coastal aquifers, and the associated wellbeing of both local populations and natural ecosystems. In this regard, the main causes of groundwater quality deterioration can be identified in aquifer salinization (often related to sea water intrusion) and pollution, generally caused by intensive anthropogenic activities (e.g. industry and agriculture) and by the lack of adequate control of sewage and waste disposal (Zuppi 2008). The combined impact of all these phenomena leads to an increase in groundwater mineralization, affecting its quality for current and future uses (Koutsoyiannis et al. 2010; Re and Zuppi 2011). For this reason, understanding the main causes of groundwater salinization is of paramount importance in order to ensure adequate water quality protection measures, and to avoid potential health and food security issues (Re et al. 2014; Zuppi 2008).

As many other zones along the Mediterranean basin, the Northeastern part of Tunisia is characterized by dominant agricultural activities, making the Cap Bon Peninsula one of the most important agricultural district of the country. In this area, the increasing withdrawal for urban and industrial purposes, coupled to an intensive agricultural exploitation, is causing acute groundwater scarcity issues (Sebei 2001; Hamza et al. 2010) and is severely threatening the quality of shallow groundwater. As a result, groundwater is generally unsuitable for domestic purposes (Ben Hammouda et al. 2010). In particular, as concerns groundwater quality, nitrate pollution is one of the main problems affecting the region, and thus a great challenge for current water management plans (Zouari et al. 2015; Re et al. 2017). In fact, although the intensive use of fertilizers has improved the regional agricultural production, its negative impacts on water quality have to be measured and assessed in order to promote new remediation measures. Based on a review of the available hydrogeochemical and hydrogeological data, the Grombalia aquifer (western part of Cap Bon Peninsula), has been chosen as priority area to assess the links of regional agricultural activities with aquifer overexploitation and salinization. The hydrogeological and hydrochemical conditions of Grombalia coastal aquifer have been studied in the last decennia for the crucial role of these water resources on regional development (Ben Moussa and Zouari 2011; Charfi et al. 2013; Hadj Sassi et al. 2006; Hamza et al. 2010; Sebei 2001; Tlili-Zrelli et al. 2013). The area is in fact characterized by high groundwater salinity and elevated nitrate concentrations, posing serious concerns for the local population. Nevertheless, as local population continues to exert pressure on the shallow coastal aquifer, like in many regions

along the Mediterranean basin, a more complete assessment on groundwater pollution origin is needed in order to support a more effective management of groundwater resources. Hydrogeochemical and isotopic results, coupled with a socio-economic analysis will be used to promote alternative science based management strategies to ensure a more sustainable use of available water resources in the region (Re 2015; Tringali et al. 2017). In this framework, the main objectives of this study are: (i) to assess groundwater quality and to identify the main geochemical processes contributing to water mineralization in the Grombalia shallow aquifer, (ii) to study the aquifer recharge and (iii) to investigate the impact of agricultural and anthropogenic activities on groundwater quality.

2.   Study area

The Grombalia plain is located in North-East Tunisia, in the Cap Bon peninsula, and covers a surface of about 719 Km². It is limited by the Gulf of Tunis (N), the oriental coastal plain and Abderrahman Mountain (E), the Takelsa syncline (NE), the Halloufa and Bouchoucha Mountains (W) and the Plain of Hammamet (S) (Fig. 1). The area is characterized by a semi-arid to sub-humid Mediterranean climate with an average annual rainfall value of 512 mm/year, a mean annual temperature of 18°C (minimum value in January and the maximum in August) and an intense potential evapotranspiration of 920 mm/year, due to the convergence of several climatic parameters (Charfi et al. 2013) like rainfall variability in time and space. The study area is characterized by both an intensive agricultural land use, with permanent (citrus, orange, olives, and viticulture) and annual crops (vegetables, grapes and cereals), and intensive industrial activities (e.g. agri-food and dairy industries), especially in the Northern part of the plain. Urban regions characterize the cities centers (Manzel Bou zelfa, Beni Khalled, Grombalia Bou Argoub and Soliman).

2.1.   *Geology and hydrogeology*

Previous studies (Castany 1948; Schoeller 1939; Ben Salem 1992; Ben Salem 1995) showed that Grombalia plain contains a series of marine and continental quaternary terraces, the recent terraces are located on the North of the plain, while, the old quaternary terraces outcrop on the South. A transition of formations' lithology is shown passing from continental deposits (sands, sandstones, and pebbles) toward coastal deposits in the North of the basin closed to Gulf of Tunis. Geologically, the Grombalia plain is defined as a graben oriented NW-SE. It is filled by Quaternary deposits, which is composed of alternating layers of permeable sand and relatively impervious marl layers forming a multilayered aquifer system. This graben is generated by two normal faults: the Hammamet fault, situated in the east of the plain, is oriented NE-SW and the Borj Cedria one, located in the

4

West part of the basin, is oriented NNW-SSE (Fig. 1). These faults, which appeared in the Middle Miocene, have contributed to the collapse of the Grombalia plain, giving rise to a rift (Ben Ayed 1993; Ben Salem 1995; Hadj Sassi et al. 2006). They constitute the boundaries of the study area (Ben Ayed, 1986). From a hydrogeologic point of view, this basin presents three principal aquifers interconnected between them: the confined deep aquifer (thickness about 200 m), the confined overlying (100 m) and the phreatic unconfined aquifer (40m) (Ennabli 1980). The upper unconfined aquifer is built of the Quaternary continental deposits (sand, sandstones and clayey sand); this aquifer is reposed on 15 m-thick of clay substratum (Ben Moussa and Zouari 2011). Its horizontal transmissivity ranges between 25×10^{-4} and 2×10^{-2} m²/S and the storage coefficient is about 5.5×10^{-3} (Tlili-Zrelli et al. 2013). The total exploitation has increased from 89.7 Mm³ in 1990 to 104.6 Mm³ in 2010 while the renewable resources are estimated to 51 Mm³/year which led to an overexploitation state of Grombalia shallow aquifer of about 205% (DGRE 1990-2010). In order to improve groundwater quality and quantity, recently the injection of surface water from Medjerda canal waters and the implementation of infiltration basins are adopted as artificial recharge techniques.
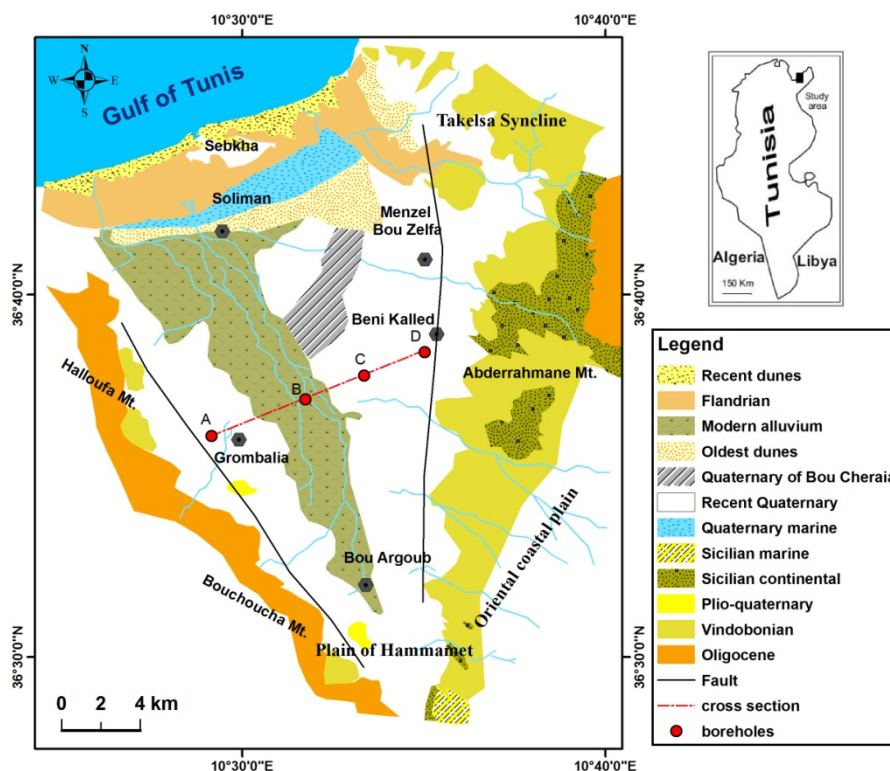

Fig. 1 Location and geological map of the Grombalia region, NE Tunisia (modified after Castany, 1948)

According to the Southwest-Northeast cross section (Fig.2), the upper aquifer is hosted in sandy Quaternary continental series captured by numerous shallow wells at depths ranging between 15 and 40 m. It is topped with

a layer of vegetal cover with a thickness of about 10 m. The deep layer is housed in Quaternary marine sandstone with an average thickness of 35 m tapped by many boreholes at depths varying from 90 to 110 m. These two aquifers constitute the main reservoir of the Grombalia hydrogeological system. Both aquifers are separated by sandy clay deposits with a thickness ranging between 30 m (SW) to 50 m (NE).
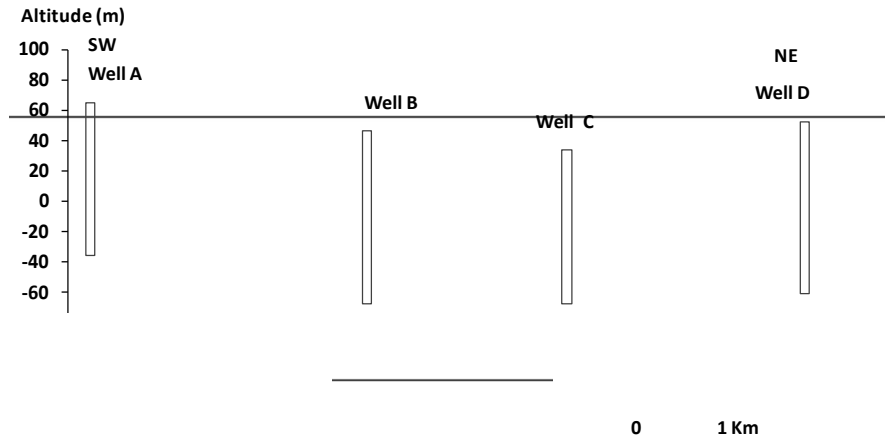

Fig. 2 Hydrogeological cross section of Grombalia basin (modified after Charfi, 2015)

2.2.   *Piezometric study*

The piezometric map of Grombalia shallow aquifer (Fig. 3a) was established based on the water level depths measurement of twenty-nine wells realized by the Regional Commissioner for Agricultural Development (CRDA) of Nabeul in 2014. The map indicates that the main groundwater flow direction is SE-NW, i.e. from the recharge area located in the South, especially in Bou Argoub region and the foothills of Abderrahman's Mountain, toward the gulf of Tunis and Sebkha el Melah as the natural discharge areas (Ennabli 1980). The piezometric map shows that the hydrostatic groundwater level progressively decreases towards the sea, with a level of 60 m in the South of Beni Khalled, to a level of 5 m in Soliman region. In addiction the comparison between the piezometric level in 1968 and 2014 (Fig. 3b) clearly shows a general decline of the groundwater level with about 10 m over a period of 47 years in Grombalia basin. Thus, the average decline is about 21 cm/year which affected almost the whole region, although the main flow direction has not changed. This lowering of the groundwater level is in relation with the deficit rainfall conditions affecting the study area and the overexploitation of groundwater reserves. The general shape of the piezometric curves in the North-eastern and North-western part of the plain was regular (in 1968) showing a flat aquifer. However, they have currently

become concave in upstream basin indicating a shift to a radial aquifer thread diverging essentially fuelled by Wadis Elbey and its effluents which can be due to the changes in land use, the overexploitation and the deviation of the flow direction of some Wadis on the surface over the years.
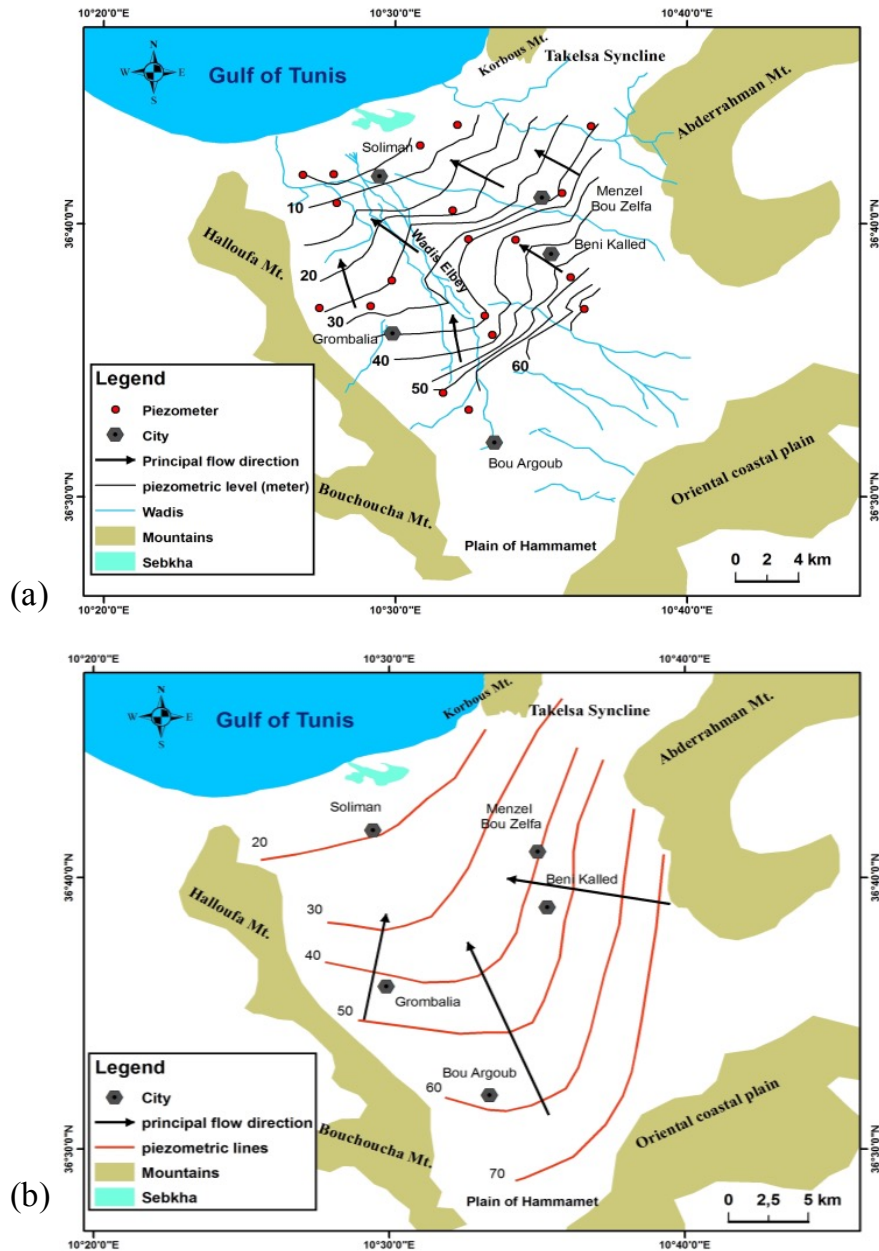

Fig. 3 Piezometric map of the Grombalia shallow aquifer (a) in 2014 and (b) in 1968 (according to Castany 1968)

3. Materials and Methods

3.1. Groundwater sampling and analyses

Between February and March 2014 a total of twenty-seven groundwater samples were collected in the Grombalia upper aquifer from wells and boreholes. All groundwater samples were analyzed for chemical and stable isotope composition at the Laboratory of Radio-Analyses and Environment (LRAE) in the National School of Engineers of Sfax (Tunisia). The measurements of temperature, pH and electrical conductivity (EC) were performed on-site for each well; major elements (Cl^-, SO_4^{2-}, HCO_3^-, NO_3^-, Na^+, Mg^{2+}, K^+, and Ca^{2+}) were analyzed by high-performance liquid chromatography (HPLC-Waters) equipped with IC–Pak TM CM/D columns for cations, using EDTA and nitric acid as eluent, and on a Metrohm chromatograph equipped with CI SUPER–SEP columns for anions, using phthalic acid and acetonitrile as eluent. The overall detection limit for ions was 0.04 mg/l. Alkalinity was analyzed in the laboratory by titration using 0.1 N HCl acid. The measurement of total dissolved solids (TDS) is performed by evaporating 100 ml of groundwater sample at 105°C during twenty-four hours. The ionic balance for all samples was within ± 5%. The spatial distribution maps of the salinity and nitrate contents were carried out using the software package of Arc GIS (Ver. 9.3). Saturation indices for halite, anhydrite, gypsum and carbonates were calculated using PhreeqC, (Parkhurst and Appelo 1999) with the software Diagrammes (Hydrogéological Laboratory of Avignon). Stable isotope analyses ($\delta18O$ and $\delta2H$) of the water samples were measured using the laser absorption spectrometer, LGR DLT 100, (Penna et al. 2010) and the results are reported in delta value expressed in ‰ versus SMOW (Standard Mean Oceanic Water). The uncertainly of stable isotopes measurements is ± 0.1 ‰ for $\delta18O$ and ±1 ‰ for $\delta2H$. Samples were analyzed for tritium contents using electrolytic enrichment and liquid scintillation counter (Taylor 1977); tritium content is expressed in tritium units (TU) with a precision of measurement equal to ± 0.3 TU.

3.2.   Geostatistical and statistical investigation

Geostatistical investigations permit to create spatial interpolation using the Kriging technique for data modeling. Ordinary Kriging method was applied in this work as surface estimator to better identify the contaminated areas and understand the spatial and temporal variability of nitrate contents and its relation with agricultural and domestic activities growth. The semivariogram is the basic geostatistic technique, and it is represented by two axes: the x-axis indicates the distance separating the pair of points that most widely varied in the input data and the y-axis represents the semi-variance $\gamma(h)$. A variogram is characterized by the following parameters (Baillargeon 2005): (i) The sill which represent the value of the variogram for the distance equal to the range, (ii) the range which means distance where two cases are different with covariance is equal to zero and (iii) the nugget effect representing the behavior of the variogram's origin reflecting the degree of spatial regularity of the

regionalized variable. If the variogram has a nugget effect, this indicates a partial lack of correlation between the values found in two close sites. It's mean that there is little resemblance between the very similar regionalized values. The semivariogram (γ(h)) is defined as half the average quadratic difference between two points separated by the distance vector (h) (Journel and Huijbregts 1978) according to the following formula:

$$\gamma(h) = \frac{1}{2N(h)} \sum_{i=1}^{N(h)} [Z(xi) - Z(xi + h)]^2$$

Where N (h) represents the total number of the variable pairs separated by this distance and z (x) is the value of the variable. For the purpose of the present study, modeling of spatial distribution of nitrate concentrations and the calculation of experimental variograms were performed using geostatistical tools integrated into Surfer 9 software (Golden Software Inc., Colorado, USA)

In addition to investigate the relation between different parameters, hydrochemical and isotopic data were statistically analyzed. Pearson's correlation matrix and principal component analysis (PCA) were applied to identify the different mechanisms that control groundwater mineralization. Principal component analysis, as one of the descriptive multivariate analysis, aims to summarize the maximum possible information by losing as little as possible of variables in order to facilitate the interpretation of a large number of initial data and to give more meaning to the reduced data (Chatfield and Collins 1980). Statistical data treatment was performed using the statistical software SPSS Statistics for Windows version 17.0. (SPSS, Inc., Chicago, USA, 2008).

4.   Results and discussion

4.1   Aquifer recharge and mineralization origin

The physico-chemical data of the analyzed groundwater samples (Table1) show a relatively wide range of temperature values, from 15.7 to 21.3°C (average 18.3°C). This variation can be related to the different water table depth and to the influence of the atmospheric temperature. The pH values range from 6.92 to 7.80 with an average of 7.21 indicating that most of samples are neutral. The average electrical conductivity is 3836 µS/cm varying within a wide range of values from 1039 µs/cm in well 23, located in the Southwestern of the plain, to 9180 µS/cm in well 1, located near to the sea shore.

The chemical composition of analyzed samples is presented in Table 1 and plotted on the Piper diagram (Piper 1944) to specify the different groundwater types of the shallow aquifer of Grombalia. When representing data on such diagram, nitrate concentrations were also taken into account, since they are not negligible due to their high values. The triangle of cations shows that the majority of samples belong to the mixed pole whereas some

groundwater samples indicate the slight dominance of calcium and magnesium. Sample 16 has the highest percentage of calcium and this can be due to cation exchange process. The triangle of anions shows the predominance of chloride and nitrate for the majority of samples except for samples No. 23 and 25 which belong to the mixed pole. The chemical data plotted in this diagram reveals the dominance the of Ca-Mg-Cl/NO_3 water type (Fig.4).
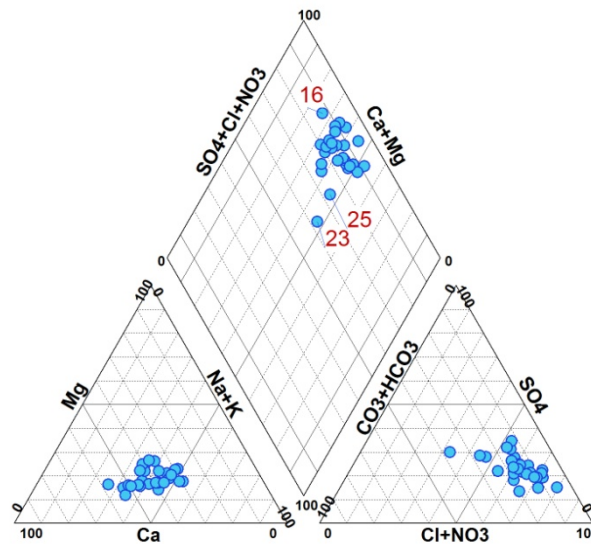

Fig. 4 Piper diagram of the Grombalia shallow aquifer

In the study region the salinity has a large variability, as demonstrated by the total dissolved solids (TDS) ranging from 715 mg/l (well 23) to 6358 mg/l (well 1), with an average of 2594 mg/l. This indicates that most samples (96%) are not adequate for drinking use, having TDS concentrations exceeding 1000 mg/l (WHO 2011). The salinity distribution map (Fig. 5) shows that lower TDS values are located in the Southeastern and Western zones of the Grombalia basin, due to the possible dilution phenomena resulting from aquifer recharge in the basin borders. On the other hand, higher TDS, characterizing some samples in the center of the plain can be associated to the abundance of evaporates deposits and the presence of intensive agriculture activities. The highest mineralization occurs in the North of the basin (wells No. 1, 3, 4, 5, 8) near the salt deposits (*sebkha*) and the Mediterranean Sea shore. In addition, for agricultural use, salinity has an adverse effect on plant growth while sodium affects soil physical properties such as infiltration (Subramani et al. 2005; Kraiem et al. 2013). The distribution of salinity levels, partially conforms to the principal groundwater flow direction, may be controlled by the residence time within the aquifer.
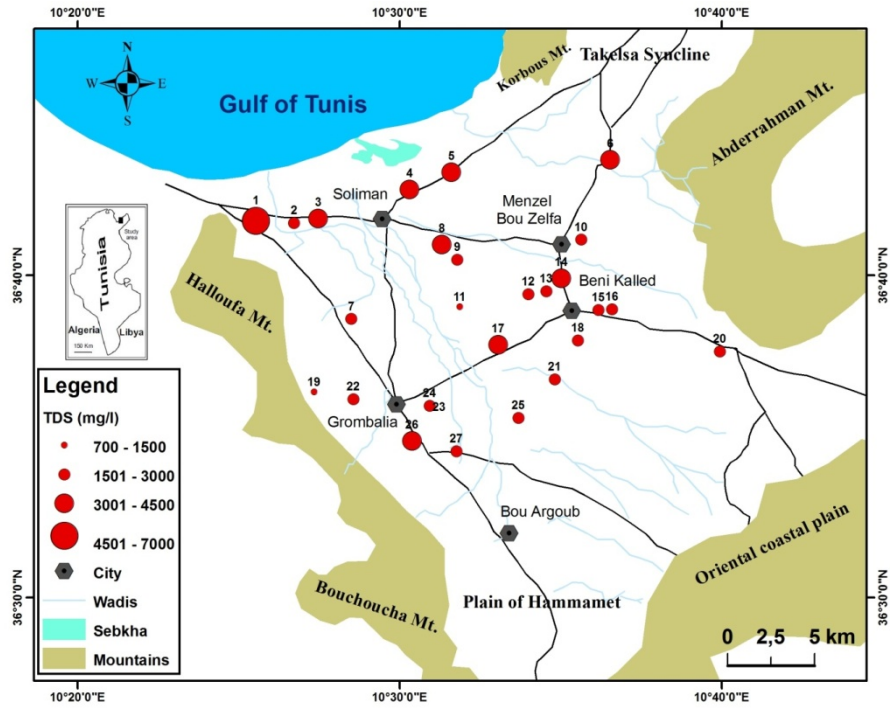
Fig. 5 Sampling and spatial distribution of the salinity in the Grombalia aquifer

Table 1 Chemical and isotopic compositions and saturation indices (SI) of groundwater samples in the Grombalia basin with descriptive statistics of all parameters

No.	T °C	pH	EC µs/cm	Cl⁻ mg/l	NO3⁻ mg/l	SO4²⁻ mg/l	HCO3⁻ mg/l	Na⁺ mg/l	K⁺ mg/l	Mg²⁺ mg/l	Ca²⁺ mg/l	TDS mg/l	Hardness mg/l	$\delta^{18}O$ (‰ Vs SMOW)	δ^2H (‰ Vs SMOW)	³H (TU)	SI Anhydrite	SI Aragonite	SI Calcite	SI Dolomite	SI Gypsum	SI Halite
1	18.0	6.96	9180	2932.4	40.5	759.6	353.8	1193.7	10.0	292.3	775.2	6358	3156	-5.4	-31.3	1.96	-0.67	0.25	0.40	0.65	-0.43	-4.17
2	21.3	7.37	2650	502.8	127.8	264.1	231.8	290.8	21.6	63.9	189.3	1692	739	-5.1	-31.9	2.42	-1.30	0.15	0.30	0.42	-1.07	-5.47
3	20.3	7.30	5720	1300.6	203.5	509.7	286.7	734.7	14.7	130.4	359.1	3539	1441	-5.2	-31.4	2.30	-0.95	0.31	0.46	0.77	-0.72	-4.7
4	18.4	7.00	5290	1450.0	419.6	723.1	292.8	585.3	28.8	147.8	610.0	4258	2142	-4.5	-28.2	1.80	-0.66	0.18	0.33	0.32	-0.42	-4.76
5	16.5	7.39	4490	815.6	465.8	554.5	329.4	422.7	35.6	93.6	395.6	3113	1379	-4.1	-25.7	2.37	-0.83	0.47	0.62	0.85	-0.59	-5.12
6	15.7	7.35	4690	893.4	85.1	610.4	414.8	530.0	0.0	86.5	405.0	3025	1373	-4.0	-24.0	2.56	-0.79	0.52	0.67	0.89	-0.54	-4.98
7	19.8	7.06	3530	661.2	155.3	296.3	414.8	298.2	17.0	111.8	302.0	2257	1221	-5.0	-29.8	1.6	-1.16	0.22	0.37	0.60	-0.92	-5.36
8	20.3	7.04	5030	1261.0	17.5	548.0	396.5	639.8	40.3	163.5	341.4	3408	1535	-4.9	-30.2	1.31	-0.95	0.17	0.32	0.61	-0.72	-4.77
9	17.5	7.27	3730	688.5	84.6	572.7	335.5	417.1	11.1	86.5	320.0	2516	1160	-3.7	-24.5	2.34	-0.87	0.30	0.45	0.57	-0.63	-5.19
10	18.2	7.13	2650	520.1	163.4	169.2	317.2	202.6	18.3	51.8	302.0	1745	971	-4.3	-29.2	1.78	-1.32	0.20	0.35	0.20	-1.08	-5.61
11	16.6	7.42	2220	415.8	0.0	366.6	164.7	274.3	13.9	50.6	146.2	1432	576	-3.5	-20.8	4.13	-1.23	-0.13	0.02	-0.18	-0.99	-5.56
12	18.7	6.92	3120	418.9	133.1	397.5	457.5	264.4	39.8	61.8	302.5	2075	1013	-4.0	-26.9	5.59	-0.99	0.12	0.27	0.11	-0.75	-5.59
13	16.6	7.20	4160	834.7	162.5	513.1	378.2	463.3	0.0	95.0	369.3	2816	1319	-3.9	-26.6	2.59	-0.88	0.32	0.47	0.59	-0.64	-5.07
14	18.2	6.92	5350	1162.8	514.7	583.6	292.8	498.4	14.6	90.2	677.4	3834	2069	-4.3	-26.2	3.76	-0.68	0.17	0.32	0.02	-0.44	-4.92
15	17.9	7.09	3860	816.2	281.8	362.4	256.2	285.5	17.4	74.3	382.9	2477	1267	-4.5	-27.3	1.22	-0.98	0.11	0.26	0.06	-0.74	-5.28
16	18.1	7.16	3680	812.9	288.3	270.5	292.8	251.6	2.5	83,0	480.0	2482	1546	-5.1	-30.2	2.69	-1.04	0.33	0.48	0.47	-0.80	-5.34
17	20.0	7.06	4400	1171.3	3.0	635.7	469.7	512.5	16.5	186.6	422.9	3418	1835	-4.5	-29.2	0.86	-0.82	0.34	0.49	0.91	-0.59	0.00
18	17.5	7.20	3440	654.7	67.0	431.2	341.6	312.0	7.9	72.3	345.0	2232	1164	-4.3	-30.2	5.21	-0.94	0.29	0.44	0.46	-0.69	-5.33
19	18.8	7.23	2390	408.8	94.2	252.9	347.7	197.9	16.8	65.5	202.7	1587	780	-4.9	-32.0	1.11	-1.28	0.19	0.33	0.45	-1.04	-5.72
20	17.2	7.27	2700	485.7	157.4	268.0	298.9	217.8	28.0	55.0	290.6	1801	956	-4.9	-29.4	2.35	-1.14	0.27	0.42	0.37	-0.9	-5.6
21	20.4	7.00	3410	733.1	132.7	345.0	292.8	351.0	20.0	90.4	198.1	2163	872	-4.7	-27.3	2.37	-1.22	-0.15	0.00	-0.05	-0.99	-5.24
22	17.9	7.61	3120	606.4	87.8	330.9	292.8	247.4	10.6	95.9	258.5	1930	1046	-4.4	-28.3	0.57	-1.14	0.54	0.69	1.20	-0.89	-5.46
23	17.7	7.80	1039	112.4	11.1	145.3	231.8	111.1	8.5	26.1	69.0	715	281	-5.4	-37.1	-	-1.77	0.20	0.35	0.53	-1.53	-6.48
24	19.4	7.16	3019	643.6	12.2	350.1	323.3	321.0	11.2	90.5	244.6	1997	989	-	-	0.00	-1.14	0.13	0.28	0.40	-0.9	-5.33
25	18.3	7.09	2770	451.7	22.4	398.1	481.9	325.1	19.1	65.5	231.8	1996	852	-4.4	-26.8	2.43	-1.09	0.19	0.34	0.40	-0.84	-5.47
26	17.6	7.23	4390	1009.6	112.6	407.2	317.2	376.1	11.2	127.7	406.5	2768	1548	-4.6	-28.5	2.41	-0.96	0.33	0.48	0.72	-0.72	-5.08
27	16.4	7.45	3550	687.6	17.7	570.2	353.8	330.6	12.7	130.7	304.5	2408	1306	-4.8	-26.3	1.49	-0.91	0.46	0.61	1.09	-0.66	-5.29
Min	15.7	6.92	1039	112.4	0.0	145.3	164.7	111.1	0.0	26.1	69.0	715	281	-5.4	-37.1	0.00	-1.77	-0.15	0.00	-0.18	-1.53	-6.48
Max	21.3	7.80	9180	2932.4	514.7	759.6	481.9	1193.7	40.3	292.3	775.2	6357	3156	-3.5	-20.8	5.59	-0.66	0.54	0.69	1.20	-0.42	0.00
Mean	18.3	7.21	3836	831.5	143.0	431.0	332.1	394.7	16.6	99.6	345.1	2594	1279	-4.5	-28.4	2.28	-1.02	0.24	0.39	0.50	-0.79	-5.07
Std.Dev	1.4	0.20	1517	525.0	140.7	162.6	74.3	216.2	10.5	53.1	155.1	1096	564.2	0.5	3.2	1.28	0.24	0.16	0.16	0.34	0.24	1.09

Table 1 shows the variability of major anions and cations contents in Grombalia basin. Accordingly, this aquifer displays higher concentrations in dissolved ions, with the highest variations observed for chloride, sulfate, nitrate, calcium and sodium contents, while the variations of bicarbonate, potassium and magnesium are rather smaller. Chloride is the predominant anion in the Grombalia aquifer. In fact, the highest Cl^- content (2932.4 mg/l) is recorded in the North of the aquifer near the coastal area suggesting the potential occurrence of anthropogenic inputs of chloride and the effects of marine aerosol spray. The nitrate contents are generally moderate to high (up to 514.7 mg/l), especially for wells No. 4, 5, 14 and 16, and with concentrations exceeding the WHO drinking-limit (50 mg/l; WHO 2011) in 70% of the wells. Sulfates show moderate levels, ranging from 145.3 to 759.6 mg/l. In this case, associated with a high content in calcium, sulfate inputs may be linked to sulfate minerals dissolution. Bicarbonate values range from 164.7 and 481.9 mg/l. Sodium contents range from 111.1 to 1193.7 mg/l. A higher variability is observed for the whole basin. The measured calcium contents show high variability with a mean of 345.6 mg/l. Generally, potassium and magnesium contents in the analyzed water samples are very low showing mainly homogenous values for the whole aquifer.

The diagram of Na^+ versus Cl^- (Fig. 6a) shows high correlation between sodium and chloride, with some points located around the dissolution line of halite (1:1 line in Fig. 6a), indicating a possible common origin of these two elements coming from halite dissolution, as explained by the reaction: ($NaCl + 2H_2O \rightarrow Na^+ + Cl^- + 2H_2O$). The dissolution process can also be highlighted, by both the under-saturation state for all samples, with respect to halite (Table 1) and the proportional parabolic correlation between the saturation indices (SI) and the sum of Na and Cl (Fig. 7a), whereas most of the points are situated under the 1:1 halite dissolution line with an excess of Cl indicating various origins of chloride. For other samples halite is highly under-saturated. Hence, it may not be the only source for Na and Cl. Sodium and chloride likely originated from surface contamination sources or saline sources (Sebkha). The diagram of Ca^{2+} versus SO_4^{2-} (Fig. 6b), shows a calcium excess for the most of samples whereas some points indicate a relative positive correlation between calcium and sulfate ($R^2 = 0.522$), that may highlight the same origin of these two elements related to the dissolution of sulfate minerals (gypsum and anhydrite). The negative saturation indices (Figs. 7b-c) of the Grombalia groundwater indicate under-saturation state with respect to the gypsum and anhydrite confirmed as well as the dissolution process of evaporates minerals. Therefore, the excess of calcium and the sodium deficiency can be attributed to cation exchange reaction that significantly affects groundwater chemical composition, by which the Na^+ cations are adsorbed by clay minerals on their surface against the release of Ca^{2+} according to the reaction: (Ca-$Clay$ $(s) + 2 Na^+ \rightarrow Na_2$ -$Clay$ $(s) + Ca^{2+}$). The cation exchange process is confirmed by the relation between $[(Ca^{2+} + Mg^{2+})$ -

$(HCO_3^- + SO_4^{2-})]$ and $[Na^+ + K^+ - Cl^-]$ examined in Figure 6d (Garcia et al. 2001). The $[(Ca + Mg) - (SO_4 + HCO_3)]$ represents the amount of calcium and magnesium gained or lost relative to that provided by the dissolution of gypsum, dolomite and calcite, whereas $[Na + K - Cl]$ values represent the amount of sodium and potassium gained or lost relative to that provided by the dissolution of halite (Fisher and Mullican 1997). These exchanges are highlighted by the sample position along a line with slope equal to -1. In the case of absence of these exchange reactions, points should be placed closed to the origin point (Abid et al. 2009; McLean et al. 2000). Figure 6d shows that majority of groundwater samples in the Grombalia basin define a straight line ($R^2 = 0.927$) with a slope of -1.27, indicating that cation exchange reactions represent a principal contributor to groundwater mineralization. Also the use of Ca $(NO_3)_2$ fertilizers increase the calcium content and contaminate the groundwater by the irrigation return flow (Stigter et al. 2006).

The diagram of Ca^{2+} versus HCO_3^- (Fig. 6c) shows a poor correlation between Calcium and bicarbonate indicating the inability of groundwater to dissolve calcite and dolomite due to the oversaturation and equilibrium states respect to these two minerals (Fig. 7d-f). Thus, Ca appears to be mainly derived from either origin like the dissolution of evaporites (anhydrite and gypsum), cation exchange process, and fertilizers.
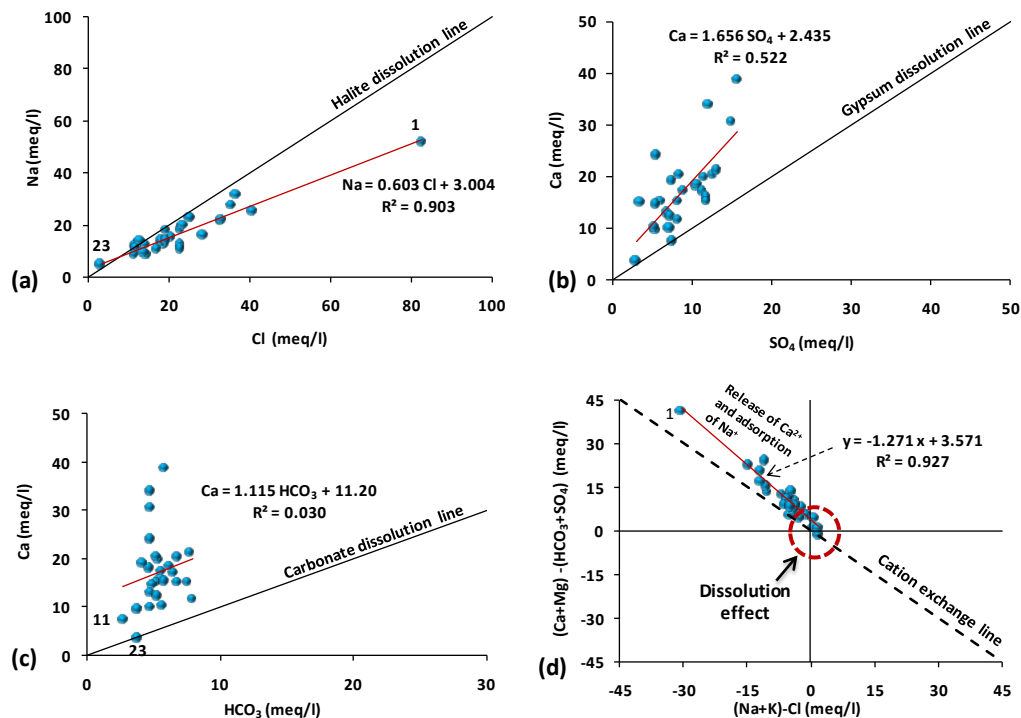

Fig. 6 Relationship between major elements: Na vs Cl (a), Ca vs SO_4 (b), Ca vs HCO_3 (c) and (Na + K) – Cl vs (Ca + Mg) - (SO_4 + HCO_3) (d).
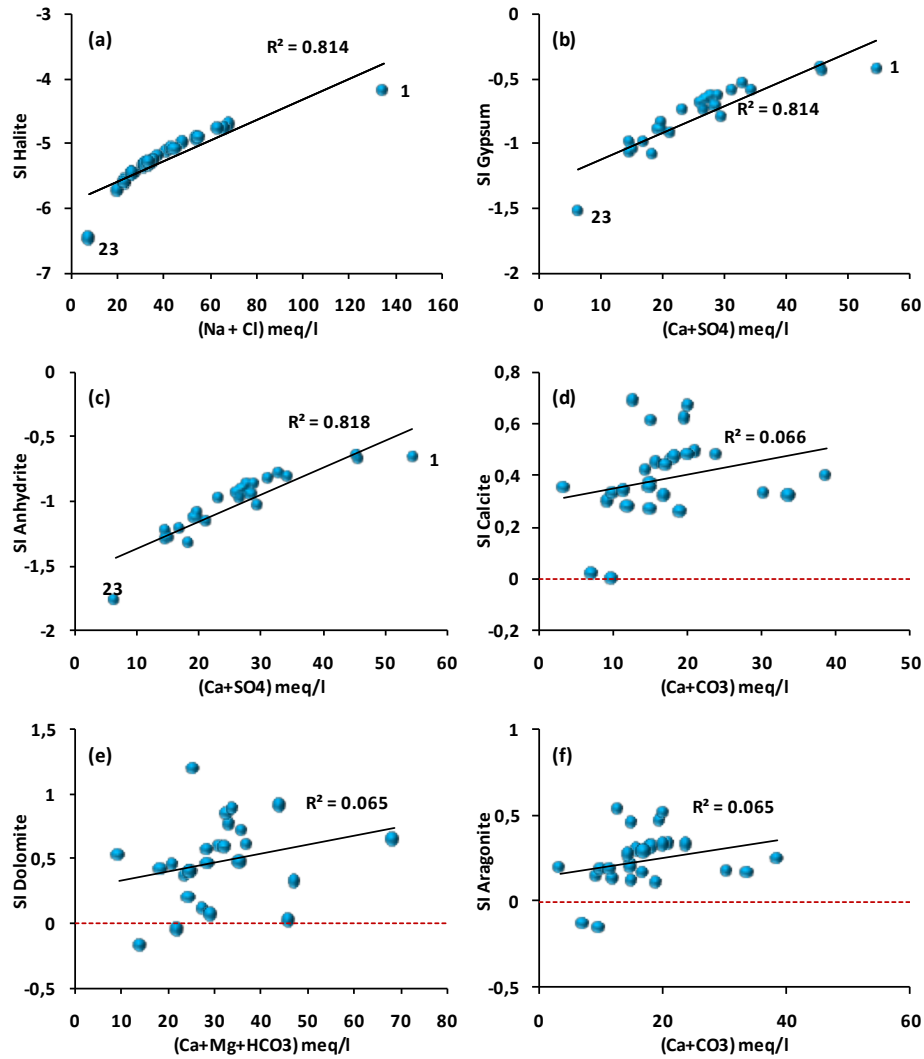
Fig. 7 Plots of (Na+Cl)/SI halite (a), (Ca+ SO₄)/SI gypsum (b), (Ca+ SO₄)/SI anhydrite (c), (Ca+CO₃)/SI calcite (d), (Ca+Mg+HCO₃)/SI dolomite (e) and (Ca+CO₃)/SI aragonite (f).

The stable isotope ratios of the water molecule range between -5.4 and -3.5 ‰ Vs. SMOW (mean of -4.5) for $\delta^{18}O$ and between -37.1 and -20.8 ‰ Vs. SMOW (mean of -28.4) for $\delta^{2}H$. Figure 8 highlights the presence of two distinct groups. The first one (G1) with the samples falling between the Global Meteoric Water Line (GMWL: $\delta^{2}H = 8.17 \delta^{18}O + 10.35$; Rozanski et al. 1993), and the Local Meteoric Water Line of Tunis-Carthage (LMWL, $\delta^{2}H = 8 \delta^{18}O + 12.4$; Zouari et al. 1985) points out the strong contribution of direct rain water infiltration to aquifer recharge, especially for points located near the hydrographic network (*Wadis*), hence confirming the rapid and recent recharge. On the other hand, the second group (G2) is characterized by samples with more enriched isotope compositions, placed below both the GMWL and the LMWL. This group corresponds to the samples dominated by an evaporation effect, according to the equation: $\delta^{2}H = 5.3 \delta^{18}O - 4.3$,

15

indicating either the slow infiltration of rainwater due to low permeable soil and/or the return flow of evaporated irrigation water.
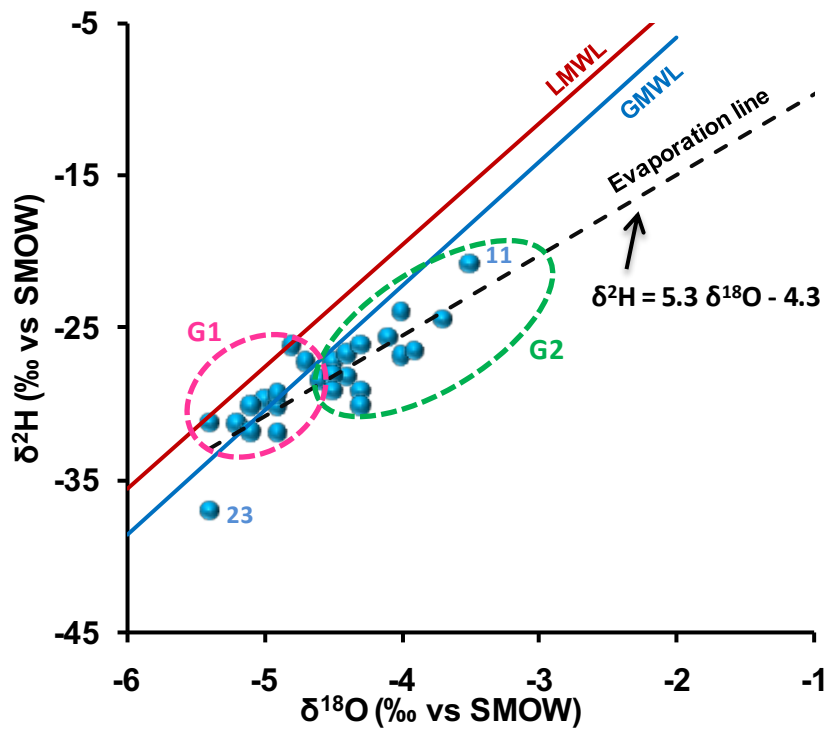

Fig. 8 Stable isotopes composition of groundwater samples in the Grombalia basin. Blue line corresponds to Global Meteoric Water Line (GMWL: $\delta^2H = 8.17 \delta^{18}O +10.35$; Rozanski et al. 1993), red line corresponds to Local Meteoric Water Line of Tunis-Carthage (LMWL, $\delta^2H = 8 \delta^{18}O + 12.4$; Zouari et al. 1985) and dashed black line represents the evaporation affect

The diagram of Cl⁻ versus $\delta^{18}O$ (Fig. 9) permits to confirm the presence of two main processes contributing to the mineralization of the shallow Grombalia aquifer: (i) dissolution of evaporative rocks, dominated by the previously described water-rock interactions, (ii) and evaporation. In fact, some samples show an isotopic enrichment, designated by the dashed black arrow in Figure 9, confirming that evaporation process contributes to groundwater mineralization.
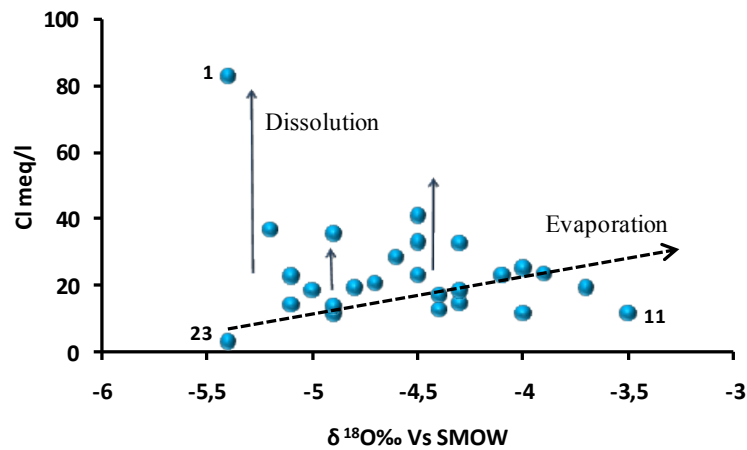
Fig. 9 Plot of Cl$^-$ versus δ ^{18}O, dashed black arrow corresponds to trend of isotopic enrichment

Tritium (^{3}H) contents in groundwater provide an indication of young groundwater ages (Dulinski et al. 2003). Its short half-life (about 12.4 years) allows it to be used as a good tool to identify recent (<50 years) water recharge (Mann et al. 1982). It depends mainly on the initial atmospheric concentration when recharge is started and the radioactive decay during infiltration from surface to saturated zone (Maduabuchi et al. 2006). The tritium activities for Grombalia water samples varies between 0 (well 24) and 5.59 (well 12) TU with an average of 2.28 TU. Considering tritium half-life and the tritium contents characterizing the precipitation in Tunisia during the nuclear tests in the middle of the last century, the ^{3}H contents above 2.0 TU likely present post-nuclear water recharge during the last 50 years or at least some components of water has been recharged in this period. In fact, high tritium contents, which characterize the Southeastern part of Grombalia basin, the recharge area, can be attributed to recent rainfall infiltration. Waters with tritium activities below 2 TU represent the pre-nuclear recharge, before the thermonuclear tests in 1950s and 1960s or the existence of mixture between recent and old waters. As it is shown on ^{3}H versus δ^{18}O diagram (Fig. 10), tritium contents in most of analyzed groundwater exceed 0.65 TU except for wells No. 22 and 24. The presence of detectable activities of tritium in groundwater highlights the modern infiltration of rainwater in this aquifer (Clark and Fritz 1997). In fact, the recent recharge signature is significant in the most of samples with enrichment of δ^{18}O isotopic composition and high ^{3}H activities observed in Grombalia shallow aquifer. Samples with highest tritium contents (No. 11, 12, 14 and 18) reflect the direct and rapid rainwater infiltration whereas the other samples (except No. 22 and 24) characterized the slow and indirect water infiltration.
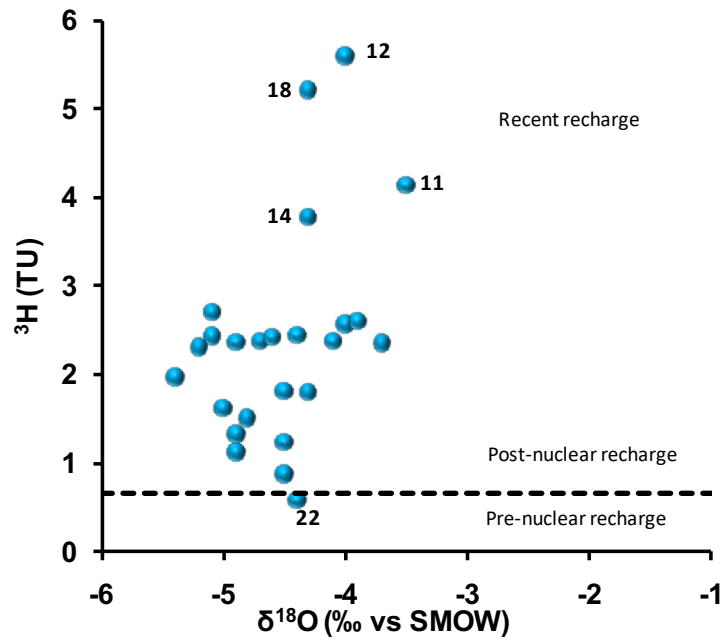
Fig. 10 Relation between δ ^{18}O and ^{3}H in groundwater samples of Grombalia basin

4.2   *Evaluation of water quality*

Groundwater quality assessment is an important issue in hydrochemistry. Variation of water quality is a function of physical parameters and chemical composition that are greatly influenced by geological nature of the reservoir and anthropogenic activities (Subramani et al. 2005). Water hardness is a commonly known as an aspect of water quality, being a measure of the concentrations of magnesium and calcium that are present in water. The standard level of hardness according to World Health Organization (WHO 2011) is 200 mg/l. The hardness of the collected samples is quite high ranging from 281 mg/l to 3156 mg/l (Table 1). It can indicate that water flowing through aquifer formations; dissolve these Ca and Mg minerals that make water harder according the flow paths, also the excessive use of $Ca(NO_3)_2$ and $MgSO_4$ fertilizers may increase water hardness highlighting the indirect role of nitrate fertilizers, inducing an acidic perturbation of the solution which is buffered by carbonate dissolution, leading to an increase in water hardness (Spruill et al. 2002). According to these high levels, the consumption of this water can have negative consequence for human health.

For nitrate contents, the majority of samples collected in the shallow aquifer show high nitrate concentrations and about 70 % of the total exceeds the statutory limit for drinking water 50 mg/l (WHO 2011). Concentrations range from 0 mg/l (well 11) to 514.7 mg/l (well 14) with an average value of 143 mg/l. Figure 11 shows that the highest concentrations are found in Beni Kalled, Menzel Bou Zelfa and Soliman regions where agricultural activities (especially irrigated agriculture) are dominant and where the groundwater static levels are close to the

18

surface (water table levels < 7m), increasing the potential for contamination by the return flow of irrigation water. Indeed, this highlights the strong link between nitrate contamination and the intensive use of fertilizers, sometimes associated to the irrigation with treated waste water, like in Soliman region, and industrial activities (e.g. agri-food and dairy industries) (Ben Moussa and Zouari 2011; Re et al. 2017). The presence of these high nitrate concentrations can be harmful for human health (Suthar et al. 2009) potentially resulting in stomach cancer for adults and methemoglobinemia in infants (Spalding and Exner 1993). On the other hand, moderate NO_3^- contents characterize the center of the study area, and relatively low nitrate concentrations distinguish Grombalia bare soils. The lower nitrate contents for some samples can be explained by either the dilution phenomenon by fresh water infiltration or denitrification process. As Grombalia is one of the most important agricultural peri-urban region in the North of Tunisia, the local nitrate contamination is therefore explained by both the intensive agriculture (i.e. excessive use of synthetic fertilizers) and domestic activities (i.e. septic system effluents and manure) which leads to increase nitrate leaching (Re et al. 2017).
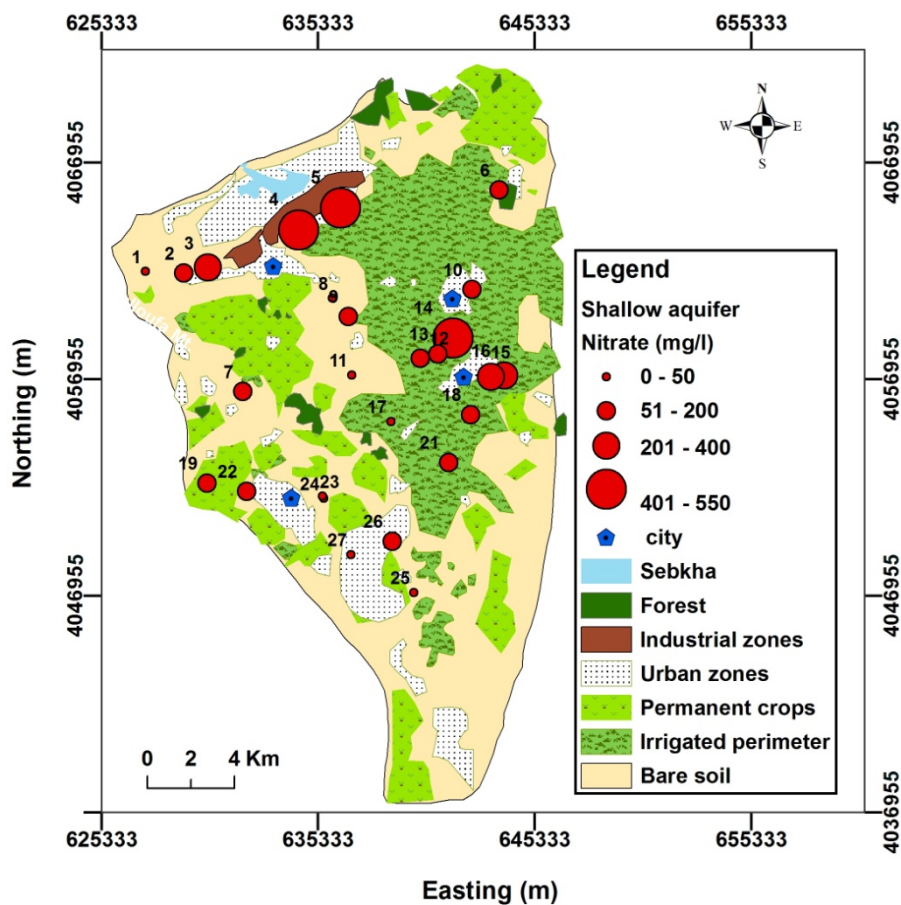

Fig. 11 land use map and distribution of nitrate concentrations (according to Chenini et al. 2015; CRDA 2016)

To compare the nitrate distribution temporally and spatially, geostatistics tools have been used. For nitrate distribution mapping, the cubic model is the most suitable experimental variogram for both 2005 and 2014 years. The variogram of 2014 is defined by the following parameters (i) The Sill is equal to 18000: for this value the covariance becomes zero; (ii) the range is equal to 8400 m. For this distance, there is an absence of correlation between two points; and (iii) the nugget effect is zero. The absence of nugget is an indication of the absence of discontinuity at the origin, reflecting the local regularity of the distribution of nitrate concentrations. For nitrate distribution map in 2005, the corresponding variogram is defined by the following parameters: (i) the sill is equal to 7800, (ii) the range is about 8500 m: this value approaches the value that obtained in 2014; and (iii) the nugget effect equals to 2000: the large value of nugget is an indication of the presence of a discontinuity at the origin. This proves that nitrate distribution in 2005 is more irregular than in 2014.

The spatial distribution of nitrate in 2014, using ordinary kriging method, (Fig. 12a) reveals that high nitrate values increased from South to North of the plain (from the recharge zone to discharge area) characterizing a SE-NW nitrate flow direction which is similar to the principal flow direction of the aquifer.

The comparison of nitrate contamination state from 2005 to 2014 (Fig. 12) reveals a remarkable reduction in nitrate levels over time, especially in the center of the plain (urban region), and an increase of nitrate concentrations in the Northeast and North parts (agricultural regions). In 2014, nitrate values in the center of the basin are below 20 mg/l whereas in 2005 the same area was characterized by a peak of nitrate pollution (up to 400 mg/l). This also coincides with the salinity decrease resulting from the use of river water *(Wadis)* for irrigation and artificial recharge (Tlili-Zrelli et al. 2013) and could be also due to the occurrence of denitrification process resulting in a depletion of nitrate content (Boettcher et al. 1990; Mengis et al. 1999; Yuan et al. 2012; Charfi et al. 2013). This comparison confirms groundwater quality changes over time and space, mainly due to soil occupation, aquifer recharge and pollutant transfer flow's rate. Indeed, this also highlights the need to set and maintain groundwater quality monitoring network to support the implementation of effective management strategies in the long-run, especially in zones where shallow aquifers represent the main source of water supply for the local population, as in the case of arid and semi-arid regions.
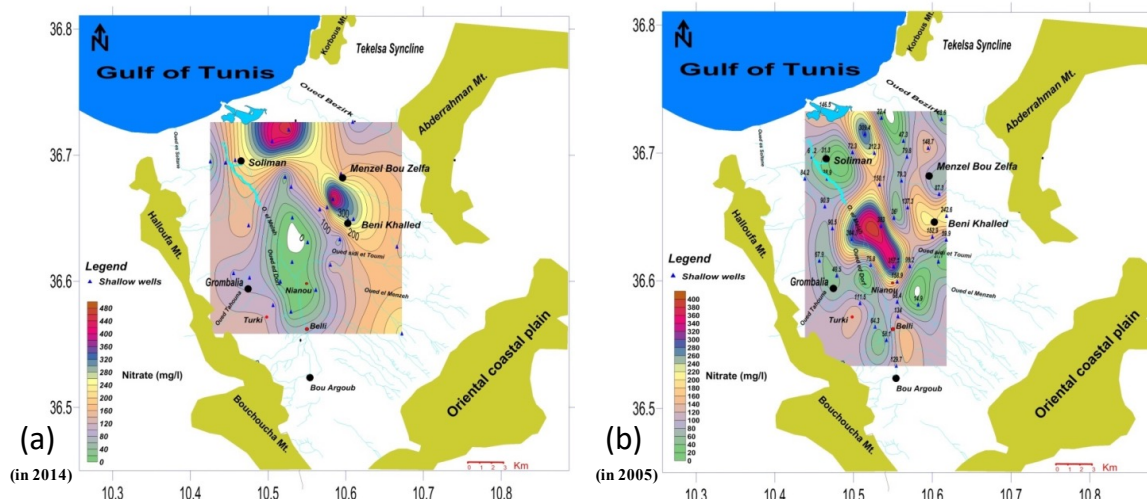
Fig. 12 Spatial distribution of nitrate using Kriging as a method of interpolation (a) in 2014 and (b) in 2005

4.3. Statistical *data treatment*

The Pearson's correlation matrix (Table 2), showing the relationship between 11 variables (Cl⁻, NO₃⁻, SO₄²⁻, Na⁺, Mg²⁺, Ca²⁺, TDS, δ^{18}O, δ^2H, EC and Hardness), indicates that: (i) high correlation ($R^2 > 0.8$) registered between Cl⁻, Na⁺, Mg²⁺, Ca²⁺, SO₄²⁻ and TDS reflects the significant contribution of these elements to the acquisition of water mineralization; (ii) the high correlation between Na⁺ and Cl⁻ ($R^2 = 0.95$ and $p < 0.05$) indicates that the dissolution of halite is an important process of mineralization; (iii) the positive correlation between Ca²⁺ and NO₃⁻ ($R^2 = 0.50$ and $p < 0.05$) shows the effect of nitrogen fertilizers; and (iv) the high correlation between Ca²⁺ and SO₄²⁻ ($R^2 = 0.72$ and $p < 0.05$) shows the dissolution of sulfate minerals.

Table 2 Pearson's correlation matrix of chemical and isotopic parameters, values marked in bold are significant (with significance level, $p < 0.05$)

		Cl⁻	NO₃⁻	SO₄²⁻	Na⁺	Mg²⁺	Ca²⁺	TDS	δ^{18}O	δ^2H	EC	Hardness
	Cl⁻	1										
	NO₃⁻	0.14	1									
	SO₄²⁻	**0.74**	0.17	1								
	Na⁺	**0.95**	0.05	**0.80**	1							
Correlation index (R²)	Mg²⁺	**0.92**	-0.08	**0.74**	**0.88**	1						
	Ca²⁺	**0.84**	**0.50**	**0.72**	**0.73**	**0.69**	1					
	TDS	**0.97**	0.28	**0.84**	**0.94**	**0.89**	0.90	1				
	δ^{18}O	-0.28	0.09	0.20	-0.19	-0.32	-0.07	-0.15	1			
	δ^2H	-0.06	0.14	0.36	0.01	-0.09	0.09	0.06	**0.85**	1		
	EC	**0.97**	0.24	**0.80**	**0.95**	**0.88**	**0.87**	**0.98**	-0.17	0.05	1	
	Hardness	**0.94**	0.31	**0.78**	**0.85**	**0.87**	**0.96**	**0.97**	-0.17	0.03	**0.94**	1

Hydro-chemical and isotopic data were analysed and interpreted using the principal component analysis (PCA) as an extraction method helpful for groundwater quality evaluation. Three principal components (with eigenvalues >1) were selected to explain 94.515% of the total variance (65.278% for F1, 18.841% for F2 and

10.396% for F3: Table 3) which conform to Kaiser-Meyer-Olkin (KMO) and Bartlett's test conditions. The KMO measure of sampling adequacy is about 0.749 and Bartlett's test of sphericity is equal to zero. These two parameters ensure that the necessary conditions of the PCA are satisfied. According to the obtained results, the first factor (F1) represents groundwater salinity due to the highly positive loading of TDS, EC, Hardness, Na^+, Cl^-, Ca^{2+}, SO_4^{2-} and Mg^{2+} (Fig. 13). This factor indicates the main geochemical process that contributed to the mineralization of groundwater defined by water-rock interactions such as dissolution of evaporites (gypsum, anhydrite and halite) and cation exchange process. High positive loadings for $\delta^{18}O$ and δ^2H designated the second factor as the evaporation component (F2) and high positive loadings for NO_3^- defined the third factor as the nitrate pollution factor (F3). The obtained results of the PCA permit to support the evidences of hydrochemical and isotopic analyses relative to the identification of the main processes contributing to groundwater salinization. Water-rock interactions, evaporation and nitrate pollution are the main mechanisms governing groundwater chemistry in the Grombalia shallow aquifer.

Table 3 Loadings of 11 variables on three significant factors (F1, F2 and F3) and total variance explained

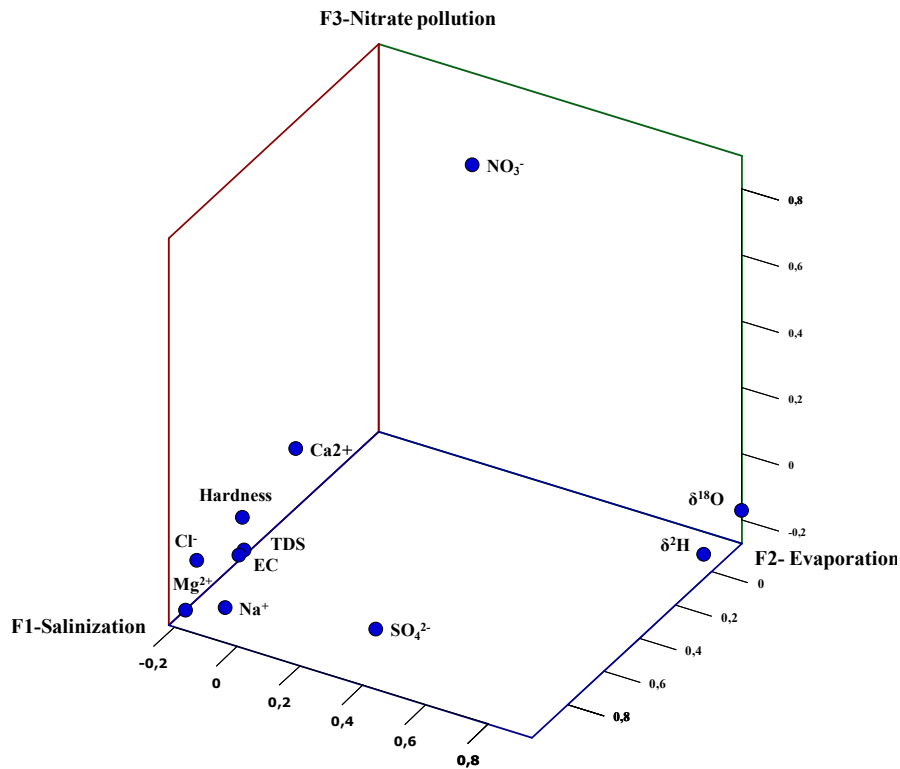|	F1	F2	F3
TDS	**0.998**	0.023	0.027
EC	**0.985**	-0.002	-0.002
Hardness	**0.975**	0.004	0.110
Cl^-	**0.974**	-0.142	-0.063
Na^+	**0.940**	-0.071	-0.202
Mg^{2+}	**0.905**	-0.218	-0.271
Ca^{2+}	**0.902**	0.132	0.317
SO_4^{2-}	**0.843**	0.352	-0.193
δ^2H	0.045	**0.938**	-0.195
$\delta^{18}O$	-0.169	**0.936**	-0.171
NO_3^-	0.246	0.318	**0.899**
Eigenvalues	7.181	2.072	1.144
% of variance	65.278	18.841	10.396
Cumulative %	65.278	84.119	94.515

Fig. 13 Component loadings plot for F1 – salinization, F2 – evaporation and F3 – nitrate pollution

The projection of all samples according to their factor scores (Fig. 14) also permits to support geochemical evidences. The most mineralized groundwater samples (quadrants I, Figs. 14a and 14b) highlight the contribution of water-rock interactions and mineral dissolution processes to the increase of water salinity. These same samples (No. 1, 8, 17 and 26) are located on the negative sides of F2 and F3 axes (quadrants IV, Fig 14c) and characterizing the most isotopically depleted samples. This indicates the absence of evaporation process due to the low interaction with the atmosphere. Also these samples are negatively correlated with NO_3 identifying the presence of denitrification process. This phenomenon is responsible of the biological transformation of NO_3^- to N_2 causing the decrease of nitrate concentration in groundwater.

In the plot of F1-salinization versus F3-nitrate pollution (Fig. 14b), different groups can be distinguished. Samples with high scores of F3 (II and III quadrants, Fig. 14b), highlight the occurrence of nitrate pollution causing by nitrogen fertilizers leaching for samples (No. 4, 5 and 14), located in the agricultural regions, and from septic tanks and manure contamination for samples No. 15, 16, 3, 2 and 26 which are situated in the urban regions, confirming the previous study presented by Re et al. (2017) and based on a complete nitrate vulnerability assessment to evaluate all the possible anthropogenic pollution sources using nitrate isotopes. Groundwater samples with high scores in F1 and low scores in F3 are characterized by high salinization rather

than nitrate pollution (quadrant I, Fig. 14b), whereas for quadrant IV (samples No. 9, 11, 12, 22 and 25) neither salinization effect nor nitrate pollution are responsible of groundwater chemical composition. According to Figs.14a and 14c these last samples, situated in the center of Grombalia basin, are affected by evaporation process characterizing by the most enriched isotopic signature ($\delta^{18}O$ and δ^2H). Groundwater samples (No. 4, 5 and 14), located on the positive sides of F1, F2 and F3 axes, characterizing by the higher nitrate values, an enrichment on isotopic composition ($\delta^{18}O$ and δ^2H) and high salinity. This highlights that groundwater chemistry for these samples are dominated by irrigation return flow which is affected by three processes (water-rock interactions, evaporation and nitrate pollution).
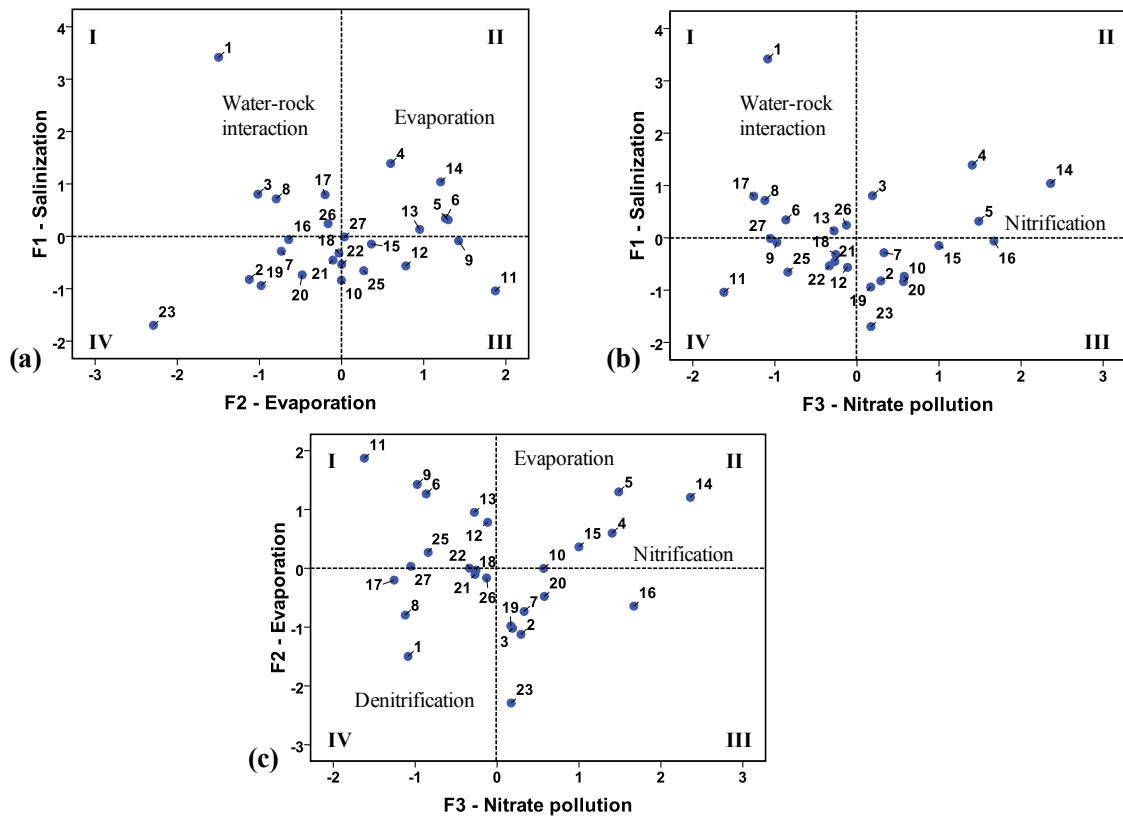

Fig. 14 Distribution of the Grombalia groundwater samples according to their scores for F1 – Salinization, F2 – Evaporation and F3 – Nitrate pollution. (a) F2 versus F1; (b) F3 versus F1 and (c) F3 versus F2

Conclusions

Hydro-geochemical, isotopic and geostatistical investigations performed in Grombalia shallow aquifer (North-eastern Tunisia), permitted to better define groundwater chemical composition, to determine the main processes contributing to aquifer mineralization and to preliminary assess the impact of human activities on groundwater quality. The hydrochemical data from the present study show that the shallow groundwater is essentially

characterized by Ca-Mg-Cl/NO$_3$ water type. Aquifer salinization is mostly due to natural processes like water-rock reactions, ion exchange and the dissolution of evaporate minerals such halite, gypsum and anhydrite. However, high nitrate contents (exceeding 50 mg/l), characterizing the majority of the samples, are mainly caused by the anthropogenic activities (e.g. agriculture and domestic uses), possibly associated to agricultural return flow and the widespread use of nitrogen fertilizers. The stable isotope composition of water reveals the existence of two different groups: (i) the first one characterized by a strong contribution of modern precipitation to aquifer recharge, confirming the recent recharge by rapid infiltration of rainwater, (ii) whereas the second group corresponds to the samples dominated by an evaporation effect, indicating either the slow infiltration of rainwater and the return flow of evaporated irrigation water. Ordinary kriging is applied to describe spatial and temporal behavior of nitrate concentrations data. Nitrate contamination occurred most in the east of the region because of nitrate excess from land use and agricultural production. Principal component analysis (PCA) is in agreement with the findings of the geochemical and isotopic assessment highlighting the geochemical processes contributing to groundwater mineralization (water rock interactions, evaporation effect and nitrate pollution). Results also highlight the need for a more rational and effective management of groundwater resources in the Grombalia region, protecting it from contamination risks (i.e. nitrate pollution, salinization), and quality degradation. In this framework, ongoing investigations involve the application of nuclear techniques to improve the understanding of the studied aquifer system, especially in relation to the interactions between the shallow and the deep aquifers and to evaluate its vulnerability to seasonal variations.

Overall current findings are very useful to promote effectiveness of the integrated approaches to tackle the key issues faced by coastal aquifers in arid and semi-arid regions (e.g salinization, contamination, and overexploitation) and to support the correct water resources protection in the long-run by promoting science base-management practices.

References

Abid K, Trabelsi R, Zouari K, Abidi I (2009) Caractérisation hydrogéochimique de la nappe du Continental Intercalaire (sud tunisien) Hydrological Sciences–Journal–des Sciences Hydrologiques, 54 (3), 526-537

Baillargeon S (2005) Le krigeage : revue de la théorie et application µa l'interpolation spatiale de données de précipitations. Maitrise en statistique pour l'obtention du grade de Maitre en sciences. Faculté des études supérieures de l'Université Laval. p 20-21.

Ben Ayed N (1986) Evolution tectonique de l'avant-pays de la chaine alpine de la Tunisie du début de Mésozoïque a` l'actuel. Thèse de Doctorat es-Science, Univ, Paris Sud. Orsay 347.

Ben Ayed N (1993) Evolution tectonique de l'avant-pays de la chaîne alpine de la Tunisie du début du Mésozoïque à l'Actuel. Thèse d'État Uni. Paris-11, Orsay, Publ. Office Nat. Mines Tunis.

Ben Hamouda MF, Tarhouni J, Leduc C, Zouari K (2010) Understanding the origin of salinization of the Plio-quaternary eastern coastal aquifer of Cap Bon (Tunisia) using geochemical and isotope investigations. Environ Earth Sci J 63:889-901.

Ben Moussa A, Zouari K (2011) Hydrochemical Investigation of Groundwater Contamination in the Grombalia Shallow Aquifer, Cap Bon Peninsula, Tunisia: Impact of Irrigation with Industrial Waste Water, Waste Water - Evaluation and Management, Prof. Fernando SebastiÃ ¡nGarcÃaEinschlag (Ed.), ISBN: 978-953-307-233-3, InTech.

Ben Salem H (1992) Contribution à la connaissance de la géologie du Cap Bon: stratigraphie, tectonique et sédimentologie. Thèse 3éme cycle, Géol. Univ. Tunis II.

Ben Salem H (1995) Evolution de la péninsule du Cap Bon (Tunisie orientale) au cours du Néogène. Notes du Service Géologique de Tunisie 61, 73-84.

Boettcher J, Strebel O, Voerkelius S, Schmidt HL (1990) Using isotope fractionation of nitrate-nitrogen and nitrate-oxygen for evaluation of microbial denitrification in a sandy aquifer. Journal of Hydrology 114, 413-424.

Castany G (1948) Les fosses d'effondrement de Tunisie. Géologie et hydrogéology. 1°fasc. Plaine de Grombalia et cuvettes de Tunisie orientale. Ann. Mines et Géol. Tunis, N_ 3, pp 18–39.

 Castany G (1968) Traité pratique des eaux souterraines. Ed Dunod, Paris, 2ème édition, p 471.

Charfi S, Zouari K, Feki S, Mami E (2013) Study of variation in groundwater quality in a coastal aquifer in NortheasternTunisia using multivariate factor analysis, Quaternary International 302, 199-209.

Charfi S (2015) Etude hydrogéologique, hydrochimique et isotopique du système aquifère de Grombalia, cap bon, Tunisie Nord-Orientale. Thèse d'état Uni. Sfax, Tunisie. p50.

Chatfield C, Collins AJ (1980) Introduction to multivariate analysis. London: Chapman and Hall. p. 256

Chenini I, Zghibi A, Kouzana L (2015) Hydrogeological investigations and groundwater vulnerability assessment and mapping for groundwater resources protection and management: state of the art and a case study. J. Afr. Earth Sci. 109, 11–26.

Clark I, Fritz P (1997) Environmental Isotopes in Hydrogeology, Lewis Publishers, New York

CRDA (2016) Commissariat Régional du Développement Agricole, carte d'occupation du sol de la plaine de Grombalia**.**

DGRE (1990–2010) General Direction of Water Ressources, annuaires d'exploitation des nappes phréatiques en Tunisie

Dulinski M, Rozanski K, Kania J, Karlikowska J, Korczynski-Jackowicz M, Witczak S, Mochalski P, Opoka M, Sliwka I, Zuber A (2003) Groundwater dating with Sulfur hexafluoride: Methodology and Field Comparison with Tritium and Hydrodynamic Methods. International Symposium, International Atomic Energy Agency, Vienna, Austria, IAEA-CN-104/8

Edmunds WM (2009) Palaeoclimate and groundwater evolution in Africa-implications for adaptation and management. Hydrological Sciences Journal 54:781–792

Ennabli M (1980) Etude hydrogéologique des aquifères du Nord-Est de la Tunisie pour une gestion intégrée des ressources en eau .Thèse de Doctorat d'Etat. Nice, p 570

Fisher SR, Mullican WF (1997) Hydrochemical evolution of sodium-sulfate and sodium-chloride groundwater beneath the Northern ChihuahuanDezert, Trans-Pecos, Texas, USA. Hydrogeology Journal 5 (2), 4-16

Garcia MG, Del Hidalgo M, Blesa MA (2001) Geochemistry of groundwater inthe alluvial plain of Tucuman province, Argentina. Hydrogeology Journal 9,597-610

Giordano M (2009) Global groundwater? Issues and Solutions. Annual Review of Environment and Resources 34(1):153–178

GWP (2012) Global Water Partnership. Water Demand. Management: The Mediterranean Experience. TECHNICAL FOCUS PAPER ISBN: 978-91-85321-88-9

Hadj Sassi M, Zouari H, Jallouli C (2006) Contribution de la gravimétrie et de la sismique réflexion pour une nouvelle interprétation géodynamique des fossés d'effondrement en Tunisie : exemple du fossé de Grombalia,C. R. Geoscience 338 751–756

Hamza MH, Maâlej A, Ajmi M, Added A (2010) Validity of the vulnerability methods DRASTIC and SI applied by GIS technique to the study of diffuse agricultural pollution in two phreatic aquifers of a semi-arid region (Northeast of Tunisia).AQUAmundi - Am01009: 057 – 064

Journel A and Huijbregts CJ (1978) *Mining Geostatistics*; Academic Press: New York, NY, USA, 1978

Koutsoyiannis D, Kundzewicz ZW, Watkins F, Gardner C (2010) Something old, something new, something red, something blue – Hydrological Sciences Journal, 55 (1), 1–3.

Kraiem Z, Zouari K, Chkir N, Agoune A (2013) Geochemical characteristics of arid shallow aquifers in ChottDjerid, South-western Tunisia, Journal of Hydro-environment Research, 1-14

Machiwal D, Jha MK (2015) Identifying sources of groundwater contamination in a hard-rock aquifer system using multivariate statistical analyses and GIS-based geostatistical modeling techniques. Journal of Hydrology: Regional Studies, 4, 80-110.

Maduabuchi C, Faye S, Maloszewski P (2006) Isotope evidence of paleorecharge and paleoclimate in the deep confined aquifers of the Chad basin, NE Nigeria. Science of the Total Environment 370, 467-479

Mann WB, Unterweger MP, Coursey BM (1982) Comments of the NBS tritiatedwater standards and their use. Int. J. Appl. Radiat. Isot. 33, 383–386

McLean W, Jankowski J, Lavitt N (2000) Groundwater quality and sustainability in an alluvial aquifer, Australia. In: Groundwater, Past Achievement and Future Challenges (ed. by O. Sililo et al.), 567–573. AA Balkema, Rotterdam, the Netherlands

Mengis M, Schif SL, Harris M, English MC, Aravena R, Elgood RJ, Maclean A (1999) Multiple geochemical and isotopic approaches for assessing ground water NO_3elimination in a riparian zone. Groundwater 37, 448-457

Paniconi C, Khlaifi I, Lecca G, Agiacomelli A, and Tarhouni J (2001) Modeling and Analysis of Seawater Intrusion in the Coastal Aquifer of Eastern Cap-Bon, Tunisia. Transport in Porous Media **43:** 3–28. Kluwer Academic Publishers. Printed in the Netherlands

Parkhurst DL, Appelo CAJ (1999) User's guide to PHREEQC (version 2)– A computer programfor speciation, batch-reaction, one-dimensional transport, and inverse geochemical cal- culations. U.S. Geological Survey Water Resources Investigations Report, 99-4259; p310

Penna D, Stenni B, Wrede S, Bogaard TA, Gobbi A, Borga M, Fischer BMC, Bonazza M, Charova Z (2010) On the repro- ducibility and repeatability of laser absorption spectroscopy measurements for d2H and d18O isotopic analysis. Hydrol Earth Syst Sci 7:2975–3014

Piper AM (1944) A graphic procedure in the geochemical interpretation of wateranalyses. Transactions, American Geophysical Union 25, 914-923

Re V, Zuppi GM (2011) Influence of precipitation and deep saline groundwater on the hydrological systems of Mediterranean coastal plains: a general overview, Hydrological Sciences Journal, 56:6, 966-980

Re V (2015) Incorporating the social dimension into hydrogeochemical investigations for rural development: the Bir Al-Nas approach for socio-hydrogeology. Hydrogeology, 23, 1293-1304

Re V, Sacchi E, Mas-Pla J, Menció A, El Amrani N (2014) Identifying the effects of human pressure on groundwaterquality to support water management strategies in coastalregions: a multi-tracer and statisticalapproach (Bou-Aregregion, Morocco). Science of the Total Environment. Volume 500, 211-223 DOI: 10.1016/j.scitotenv.2014.08.115

Re V , Sacchi E, Kammoun S, Tringali C, Trabelsi R, Zouari K, Daniele S (2017) Integrated socio-hydrogeological approach to tackle nitrate contamination in groundwater resources. The case of Grombalia Basin (Tunisia). Science of the Total Environment 593–594 (2017) 664–676, DOI: 10.1016/j.scitotenv.2017.03.151

Rozanski K, Araguás-Araguás L, Gonfiantini R (1993) Isotopic patterns inmodern global precip- itation. GeophysMonogr 1993;78:1–36.

Schoeller H (1939) Le quaternaire du Golfe ancien de Grombalia. Tunisie. Actes Société Linnéenne de Bordeaux 91, 14-30

Sebei A (2001) Impacts des activités anthropiques sur la qualité des eaux de la plaine de Grombalia. Diplôme d'études approfondies. Université Tunis El Manar, Faculté des sciences de Tunis

Siebert S, Burke J, Faures JM, Frenken K, Hoogeveen PD, Döll P, Portmann FT (2010) Groundwater use for irrigation – a global inventory. Hydrology and Earth System Science 14:1863–1880

Spalding RF, Exner ME (1993) Occurrence of nitrate in groundwaterea review. J. Environ. Qual. 22 (3), 392-402

Spruill TB, Showers WJ, Howe SS (2002) Application of classification-tree methods to identify nitrate sources in ground water. Journal of Environmental Quality 31: 1538-1549.

Stigter TY, Carvalho AM, Ribeiro L, Reis E (2006) Impact of the shift from groundwater to surface water irrigation on aquifer dynamics and hydrochemistry in a semi-arid region in the south of Portugal. Agric Water Manag 85:121–132

 Subramani T, Elango L, Damodarasamy SR (2005) Groundwater quality and its suitability for drinking and agricultural use in Chithar River Basin, Tamil Nadu, India Environ Geol (2005) 47: 1099–1110 DOI 10.1007/s00254-005-1243-0

Suthar S, Bishnoi P, Singh S, Mutiyar PK, Nema AK, Patil NS (2009) Nitrate contamination in groundwater of some rural areas of Rajasthan, India. J. Hazard. Mater. 171, 189-199

Taylor CB (1977) Tritium enrichment of environmental waters by electrolysis: development of cathodes exhibiting high isotopic separation and precise measurements and Applications. High Tatras, Czechoslovakia, October 1975, Bratislava (1977), pp 133–140

Tlili-Zrelli B, Hamzaoui-Azaza F, Gueddari M, Bouhlila R (2013) Geochemistry and quality assessment of groundwater using graphical and multivariate statistical methods. A case study: Grombalia phreatic aquifer (Northeastern Tunisia). Arab J Geosci 6:3545–3561 DOI 10.1007/s12517-012-0617-3

Tringali C, Re V, Siciliano G, Chkir N, Tuci C, Zouari K (2017) Insights and participatory actions driven by a socio-hydrogeological approach for groundwater management: the Grombalia Basin case study (Tunisia). Hydrogeology Journal (in press; DOI: 10.1007/s10040-017-1542-z).

UNESCO-ISARM (2004) United Nations Educational, Scientific and Cultural Organization - Internationally Shared Aquifer Resources Management Managing shared aquifer resources in Africa. B. Appelgren, ed. Paris: UNESCO IHP-VI, Series in Groundwater no 8

Van der Gun J (2012) Groundwater and Global Change: Trends, Opportunities and Challenges. UNESCO Side Publication Series 01. ISBN 978-92-3-001049-2.

WHO (2011) World Health Organization. Guidelines for drinking-water quality, fourth edition. 564p. ISBN: 978 92 4 154815 1

Yuan L, Zonghe P, Tianming H (**2012**) Integrated assessment on groundwater nitrate by unsaturated zone probing and aquifer sampling with environmental tracers. Environmental Pollution 171, 226-233

Zghibi A, **Tarhouni J**, **Zouhri L (2013**) Assessment of seawater intrusion and nitrate contamination on the groundwater quality in the Korba coastal plain of Cap-Bon (North-east of Tunisia).Journal of African Earth Sciences 87, 1–12

Zouari K, **Aranyossy JF**, **Mamou A**, **Fontes JCh (1985)** Etude isotopique et géochimique des mouvements et de l'évolution des solutions de la zone aérée des sols sous climat semi-aride (Sud tunisien). In: Stable and radiactive isotopes in the study of the unsaturated soil zone. IAEA-TECDOC-357, Vienna. p.121-144

Zouari K, Re V, Sacchi E, Trabelsi R, Kammoun S, (2015) The use of nitrate isotopes to assess agricultural and domestic impacts on groundwaterquality in rural zones. The example of Grombalia basin (Tunisia). International Symposium on Isotope Hydrology: RevisitingFoundations andExploringFrontiers; 2015 May 11-14; Vienna, Austria

Zuppi GM (**2008**) The groundwater challenge. In: Clini C, Musu I, Gullino M L (eds.), Sustainable development and environmental management Experience and case studies, DORDRECHT, Springer

List of figures captions

Fig. 1 Location and geological map of the Grombalia region, NE Tunisia (modified after Castany, 1948)

Fig. 2 Hydrogeological cross section of Grombalia basin (modified after Charfi, 2015)

Fig. 3 Piezometric map of the Grombalia shallow aquifer (a) in 2014 and (b) in 1968 (according to Castany 1968)

Fig. 4 Piper diagram of the Grombalia shallow aquifer

Fig. 5 Sampling and spatial distribution of the salinity in the Grombalia aquifer

Fig. 6 Relationship between major elements: Na vs Cl (a), Ca vs SO_4 (b), Ca vs HCO_3 (c) and (Na + K) – Cl vs (Ca + Mg) - (SO_4 + HCO_3) (d).

Fig. 7 Plots of (Na+Cl)/SI halite (a), (Ca+ SO_4)/SI gypsum (b), (Ca+ SO_4)/SI anhydrite (c), (Ca+CO_3)/SI calcite (d), (Ca+Mg+HCO_3)/SI dolomite (e) and (Ca+CO_3)/SI aragonite (f).

Fig. 8 Stable isotopes composition of groundwater samples in the Grombalia basin. Blue line corresponds to Global Meteoric Water Line (GMWL: $\delta\ ^2H$= 8.17 $\delta\ ^{18}O$ +10.35; Rozanski et al. 1993), red line corresponds to Local Meteoric Water Line of Tunis-Carthage (LMWL, δ^2H = 8 $\delta^{18}O$ + 12.4; Zouari et al. 1985) and dashed black line represents the evaporation affect

Fig. 9 Plot of Cl⁻ versus δ ^{18}O, dashed black arrow corresponds to trend of isotopic enrichment

Fig. 10 Relation between δ ^{18}O and ^{3}H in groundwater samples of Grombalia basin

Fig. 11 land use map and distribution of nitrate concentrations (according to Chenini et al. 2015; CRDA 2016)

Fig. 12 Spatial distribution of nitrate using Kriging as a method of interpolation (a) in 2014 and (b) in 2005

Fig. 13 Component loadings plot for F1 – salinization, F2 – evaporation and F3 – nitrate pollution

Fig. 14 Distribution of the Grombalia groundwater samples according to their scores for F1 – Salinization, F2 – Evaporation and F3 – Nitrate pollution. (a) F2 versus F1; (b) F3 versus F1 and (c) F3 versus F2

List of tables captions

Table 1 Chemical and isotopic compositions and saturation indices (SI) of groundwater samples in the Grombalia basin with descriptive statistics of all parameters

Table 2 Pearson's correlation matrix of chemical and isotopic parameters, values marked in bold are significant (with significance level, $p < 0.05$)

Table 3 Loadings of 11 variables on three significant factors (F1, F2 and F3) and total variance explained